Detection of inter-turn short-circuit fault in induction motor operating under varying load conditions by using the angular domain order tracking technique

Yassine MISSOUM BENZIANE **Naimi MOKHTARI**
IRECOM laboratory, Department of Electrotechnics, Djillali Liabes University of Sidi Bel-Abbes, 22000, Algeria
yassine.mbenz@yahoo.com mokhtari_n@yahoo.com

Abdelkader LOUSDAD
LMSS laboratory, Department of Mechanics, Djillali Liabes University of Sidi Bel-Abbes, 22000, Algeria
a_lousdad@yahoo.com

Abstract: *Order tracking is one among the most reliable techniques in the field of vibration analysis for condition monitoring and fault diagnosis of rotating machineries. The key of its success is due to its capability to clearly identify non-stationary vibrations, which vary in amplitude and frequency. In the present paper, the Angular Domain Order Tracking (AD-OT) technique is applied for the first time on the induction motor current signal for detecting inter-turn short-circuit (ITSC) fault and compared with the classical Fourier analysis (FFT). For this purpose, an induction motor with an ITSC fault was modelled in the Matlab/Simulink environment and numerical simulations were performed under varying load conditions. The motor current and speed were monitored with and without fault (i.e healthy and with ITSC fault), and then analysed by the AD-OT technique. The obtained results show that the presented technique is more efficient than the FFT technique, especially for the detection of the inter-turn short-circuit fault under non-stationary conditions.*

Key words: *Induction motor, Angular domain order tracking, Fault diagnosis, Inter-turn short-circuit fault.*

1. Introduction

Induction motors are key components in many industrial applications due to their construction, versatility, low cost and stable operation. However, it is crucial to have information on their behavior and condition to prevent degradation, malfunctions or failures during their operating service. Usually, induction motors operate under several types of stresses which can produce different types of faults. These faults may be classified into two groups according to their location: the stator faults and rotor faults. The stator faults are manifested by stator-winding open or a short-circuit (turn-to-turn, phase-to-phase or phase-to-stator frame). Rotor faults include rotor winding open or short-circuits for wound rotor and broken bar and/or cracked end ring faults for squirrel cage rotor [1].

According to [2, 3, 4], 30% to 40% of induction motor faults are due to defects in the stator winding. Such faults are generally due to a combination of various stresses (thermal, electrical, mechanical and environmental) acting on the stator.

Commonly, a small number of shorted turns do not have great physical signs, but it can induce a catastrophic insulation failure in a brief period of time. Early detection of ITSC fault during motor operation can prevent the occurrence of some damage in adjacent coils and stator core, therefore reducing the repair cost and motor outage time [5, 6]. For this purpose different strategies for the detection of ITSC fault in induction motor have been developed. Among them, vibration analysis [7], infrared thermography analysis [8] and motor current signal analysis (MCSA) [9] which is the most widely used due to its simplicity (requiring only one current sensor to acquire the stator current signal and a classical Fourier analysis (FFT) to obtain its spectral energy) and non-invasive properties [10, 11]. Unfortunately, although the MCSA is particularly powerful for induction motor operating under stationary conditions, it stills inadequate for a system undergoing sudden load changes [12, 13]. For this purpose another methodology is used in this kind of situation based on time-frequency distributions (TFD) techniques such as wavelet transform (WT) [12, 14] and Short Time Fourier Transform (STFT) [15]. Another interesting approach has been developed during these last years based on the so-called order tracking (OT) technique, which consists in analysing the frequencies corresponding to the motor speed or to its multiples commonly known as "orders".

The OT technique is distinguished from the TFD techniques by its precision and the simplicity of its diagnostic procedure because it allows displaying the results in a plot similar to the FFT spectrum. In [16], Akar used successfully the AD-OT technique for the detection of static eccentricity fault in a closed loop driven induction motor.

In the present work, the AD-OT technique is used for the analysis of the stator motor current signal to detect the stator ITSC fault under varying load conditions.

2. Angular Domain Order Tracking

Order tracking (OT) is considered as one among the most important techniques in vibration analysis. Its main advantage compared to other analytical techniques is its ability to clearly identify non-stationary vibration and easy noise analysis of components which vary in amplitude and frequency influenced by the rotational speed of the reference

shaft. OT can be performed by many different ways each of them presenting advantages and disadvantages. According to Blough [17] the most and widely used order tracking techniques are: the Fourier transform based order tracking (FT-OT), the angular domain order tracking (AD–OT) and the Vold-Kalman order tracking filter (VKF–OT).

The principle of the AD-OT technique consists in acquiring the data with a constant interval Δt. Then these sampled data are in their turn sampled to equal angular intervals via the use of an interpolation algorithm [17]. The times when the equal angular intervals occur are determined by two methods: either by using one tacho pulse per revolution as synchronization pulses or using the rpm-time profile (further details can be found in [18]).

The sampled data in the angular domain are processed via the FFT or Discrete Fourier Transform. The output spectral lines represent the constant orders from the moment that the transforms are realised on angular domain data. This involves that there are equivalent sampling relations in the angle/order domain to the time/frequency relation. These equivalent sampling relations are given as follow:

$$\Delta_0 = \frac{1}{R} = \frac{1}{N * \Delta\theta} \tag{1}$$

$$R = N * \Delta\theta \tag{2}$$

$$O_{nyquist} = O_{max} = \frac{O_{sample}}{2} \tag{3}$$

$$O_{sample} = \frac{1}{\Delta\theta} \tag{4}$$

where Δ_0 is the order spacing of the exiting order spectrum, R is the total number of analysed revolutions, N is the total number of points on which the transformation is performed, $\Delta\theta$ is the angular spacing of the resampled data. O_{sample}, $O_{nyquist}$ and O_{max} are respectively the angular sampling rate at which the data is sampled, the Nyquist order and the maximum order which can be analysed. This involves that the analysis must be performed on many revolutions to obtain a good order resolution. The maximum order which can be analysed can be determined via the number of samples/or the angular sampling rate per revolution. . The cores of the Fourier transforms reformulated in the angular domain are expressed in the following form:

$$a_m = \frac{1}{N}\sum_{n=1}^{N} x(n\Delta\theta)\cos(2\pi o_m n\Delta\theta)$$
$$b_m = \frac{1}{N}\sum_{n=1}^{N} x(n\Delta\theta)\sin(2\pi o_m n\Delta\theta) \tag{5}$$

where o_m, a_m and b_m represent respectively the order which is being analysed, the Fourier coefficient of the cosine term for o_m and the Fourier coefficient of the sine term for o_m.

The AD-OT technique marking flow diagram is illustrated in Fig. 1[16].

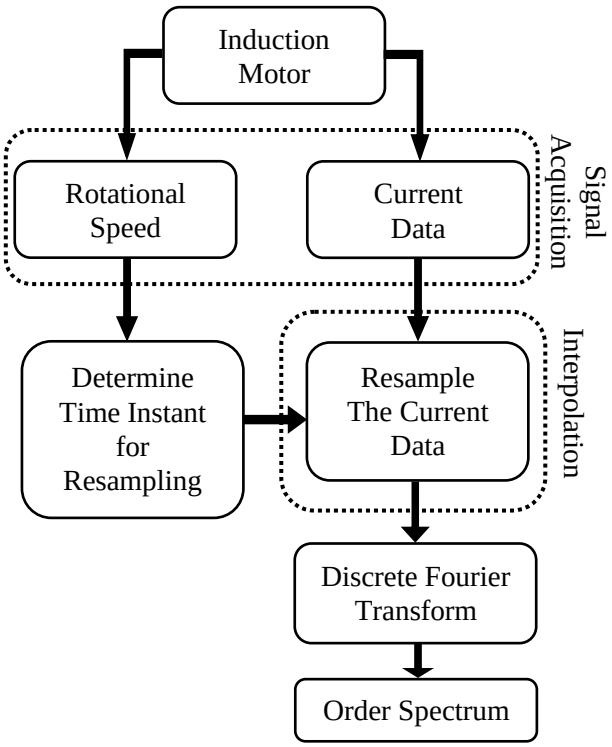

Fig. 1. Angular Domain Order Tracking technique diagram

3. Modelling of the induction machine

In this study a three-phase squirrel cage induction motor is considered. Its rotor consists of conductor bars regularly distributed at the periphery of the rotor and connected to each other by two short-circuit rings. To develop our model, the rotor cage is considered as a system of $(N_b + 1)$ Loops as shown in Fig. 2 [19, 20, 21].

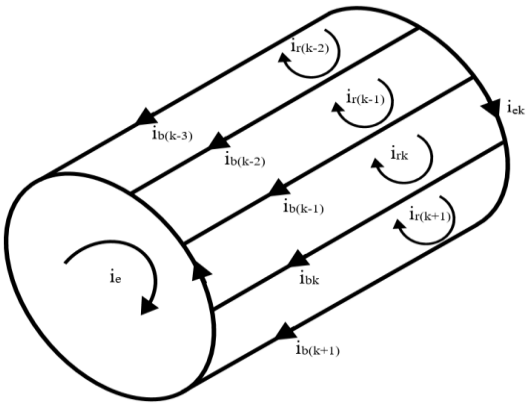

Fig. 2. Rotor model of the induction motor

Using the classical assumptions which assume that the relative permeability is infinite, the skin effect and saturation are negligible and the magneto motive force (mmf) of the stator is sinusoidally distributed. We calculate the various inductances and mutual which intervene in the equations of the circuit [19, 21, 22].

3.1. Calculations of the inductances

3.1.1. Stator inductance

The expression of mmf in a phase " a " is given as follow:

$$F(\theta)=\frac{2N_s}{\pi.p}i_{as}\cos\theta \tag{6}$$

The induction due to the stator coil of phase " a " is written as:

$$B(\theta)=\frac{2.\mu_0.N_s}{\pi.e.p}i_{as}\cos p\theta \tag{7}$$

The main flux and the cyclic inductance are given by:

$$\phi_s=\frac{4.\mu_0.N_s^2}{\pi.e.p^2}R.l.i_{as} \tag{8}$$

$$L_{as}=L_{sp}+L_{sf}=\frac{4.\mu_0.N_s^2}{\pi.e.p^2}R.l+L_{sf}$$

The mutual inductance between the stator phases is calculated as:

$$M_s=-\frac{L_s}{2} \tag{9}$$

3.1.2. Rotor inductance

The principal inductance of a rotor mesh are given as follow [14]

$$L_{rp}=\left(\frac{N_b-1}{N_b^2}\right)\frac{\mu_0}{e}2.\pi.R.l \tag{10}$$

The total inductance of the k^{th} rotor mesh as well as the mutual between two meshes are expressed as follows:

$$L_{rr}=L_{rp}+2L_b+2L_e \tag{11}$$

3.1.3. Inductance stator-rotor

The mutual inductance stator-rotor between the stator phase " a " and the rotor mesh k is given by:

$$M_{snrk}=-M_{sr}\cos(p\theta_r-n\frac{2\pi}{3}+k.\alpha) \tag{12}$$

where

$$M_{sr}=\frac{4.\mu_0 N_s R.l}{\pi.e.p^2}\sin\left(\frac{\alpha}{2}\right)$$

$\alpha=p\left(2\pi/N_b\right)$ is the electrical angle of two adjacent rotor meshes

3.2. System equation

In order to facilitate our modelling, we apply the extended Park transform to the rotor system so as to transform the N_b bars system in a (d,q) system. The obtained result can take the following canonical form:

$$L\dot{X}(t)=A(\omega)X(t)+Bu(t) \tag{13}$$

with

$$X=\left[I_{ds}\ I_{qs}\ I_{dr}\ I_{qr}\ I_e\right]^T,u=\begin{bmatrix}V_{ds}\\V_{qs}\end{bmatrix},B=\begin{bmatrix}1&0\\0&1\\0&0\\0&0\\0&0\end{bmatrix}$$

$$A(\omega)=-\begin{bmatrix}R_s&-\omega L_{sc}&0&-\frac{N_b}{2}\omega M_{sr}&0\\ \omega L_{sc}&R_s&-\frac{N_b}{2}\omega M_{sr}&0&0\\ -\frac{3}{2}M_{sr}&0&R_r&0&0\\ 0&\frac{3}{2}M_{sr}&0&R_r&0\\ 0&0&0&0&R_e\end{bmatrix}$$

$$L=\begin{bmatrix}L_{sc}&0&-\frac{N_b}{2}M_{sr}&0&0\\ 0&L_{sc}&0&\frac{N_b}{2}M_{sr}&0\\ -\frac{3}{2}M_{sr}&0&L_{rc}&0&0\\ 0&\frac{3}{2}M_{sr}&0&L_{rc}&0\\ 0&0&0&0&L_e\end{bmatrix}$$

where

$$L_{rc}=L_{rp}-M_{rr}+2(L_e/N_b)+2L_e(1-\cos\alpha)$$

$$R_r=2\frac{R_e}{N_b}+R_b\left(1-\cos\alpha\right)$$

The expression of the torque is given by:

$$C_e=\frac{3}{2}p.N_b.M_{sr}(i_{ds}.i_{qr}-i_{qs}.i_{dr}) \tag{14}$$

3.3. Modelling of the short-circuit fault

Starting from the idea proposed by [23] the ITSC fault is obtained by introducing an additional short-circuited coil whose number of turns n_{cck} is equal to the number of defected turns in the motor. Thus, in the presence of a stator imbalance, the motor contains, in addition to the stator windings and the rotor cage, a short-circuited winding at the origin of the stationary field of fixed direction θ_{cck} with respect to the stator. The state model of the induction motor taking account of the ITSC fault can be expressed by the following system of nonlinear equations as in [24, 25]:

$$\begin{cases} \dot{X}(t) = \left(A(\omega)X(t) + Bu(t)\right)L^{-1} \\ Y(t) = CX(t) + Du(t) \end{cases} \quad (15)$$

with

$$C = \begin{bmatrix} 1 & 0 & 0 & 0 & 0 \\ 0 & 1 & 0 & 0 & 0 \end{bmatrix}, D = \sum_{k=1}^{3} \frac{2}{3} \frac{\eta_{cck}}{R_s} P(-\theta) Q(\theta_{cck}) P(\theta), \eta_{cck} = \frac{n_{cck}}{n_s}$$

$$Q(\theta_{cck}) = \begin{bmatrix} cos(\theta_{cck})^2 & cos(\theta_{cck}) sin(\theta_{cck}) \\ cos(\theta_{cck}) sin(\theta_{cck}) & sin(\theta_{cck})^2 \end{bmatrix}$$

$$P(\theta) = \begin{bmatrix} \cos(\theta) & -\sin(\theta) \\ \sin(\theta) & \cos(\theta) \end{bmatrix}$$

where the matrix $Q(\theta_{cck})$ is depending on the short-circuit angle {when the ITSC occurs on phase a (respectively b and c), then the angle θ_{cck} is 0 rad (respectively $2\pi/3$ and $4\pi/3$)} and θ is the electrical angle.

4. Simulation results and discussion

In order to validate the model presented in the previous section and to evaluate its behavior in the healthy and faulty case, numerical simulations were carried out under the Matlab/Simulink environment. For this purpose, a 1.1 kW, 220 V, 50 Hz, 2-pole induction motor is used. The induction motor parameters are given in Tab. 1.

The motor is started with a symmetrical three-phase sinusoidal voltage. At instants t=0.5 s and 2 s respectively. The motor is loaded with a torque of 3 Nm and 5 Nm. At time t=4 s a dynamic load is applied which increases the load value up to 7 Nm as shown in Fig. 3. The same procedure is used when the stator presents a fault of 1 and 4 shorted turns in phase " a " introduced at the instant t=1 s.

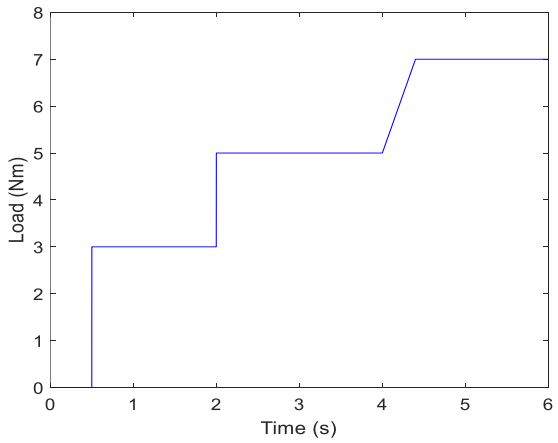

Fig. 3. Applied load to the induction motor

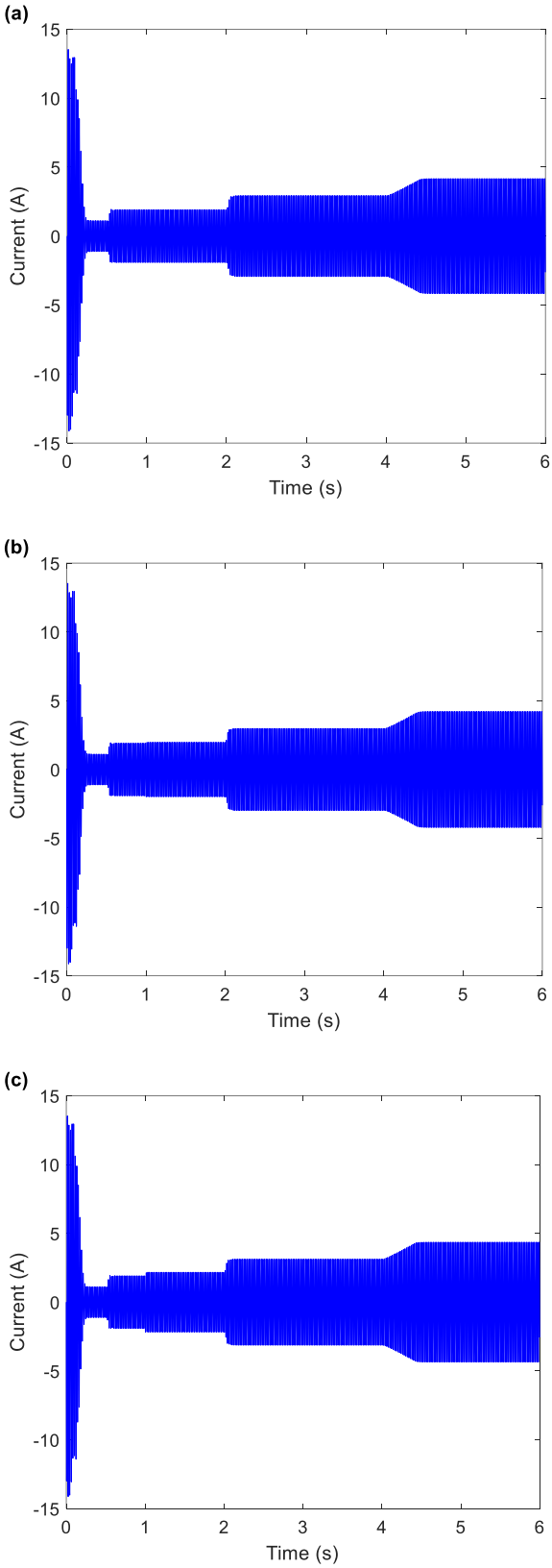

Fig. 4. Evolution of current, (a) healthy case, (b) faulty case (1 shorted turn at t = 1 s in phase a), (c) faulty case (4 shorted turns at t = 1 s in phase a)

The curves of the stator current for the healthy state, 1 shorted turn, 4 shorted turns are shown respectively in Fig. 4 (a), (b) and (c). In Fig. 4 (a) we can easily observe an increase in the amplitude of the current at instants t = 0.5 s, 2 s and 4 s corresponding to the moments when the loads are applied. In Fig. 4 (b) and (c) we notice a slight increase in the amplitude of the current at the instant t = 1 s which coincides with the moment when the ITSC fault is introduced. This increase in amplitude is much more visible in the case of 4 shorted turns as shown in Fig. 4 (c).

From these observations, it is clear that the detection of an ITSC fault using conventional analysis of the stator current in the time domain is difficult to perform especially in the cases of small number of shorted turns and load variations. Hence it is important to implement an analysis that allows exploiting all the information present in the motor current signal.

Application of the AD-OT technique to the stator current

In this section, a thorough analysis of the information present in the stator current is carried out through the application of the FFT and AD-OT techniques. The implementation of the AD-OT technique requires the introduction of several parameters such as the sampling frequency and the rotational speed information.

However, before we begin our analysis, we consider it important to know that a ITSC fault makes appear a $f_{sc_k} = k.f_s$ frequency lines near the fundamental on the stator current frequency spectrum (k = 3, 5, 7…)[12]. Therefore, the location of these frequency lines in the order domain is obtained by the equation (16):

$$Order = Frequency.\left(60 \diagup \omega_r\right) \quad (16)$$

where ω_r is the rotational speed in rpm.

The frequency spectrum of the stator current obtained with the FFT technique for different load levels are shown in Fig.5. From this figure, it can be seen that the ITSC fault induce a new frequency component with a value of $f_{sc3} = 3.f_s$ (150 Hz). For the load values of 3 Nm, 5 Nm and 7 Nm, the amplitude of this component is proportional to the number of shorted turns.

On the other hand, a decrease in the amplitude of the ITSC fault component is noted when the value of the load increases, until it becomes almost imperceptible for a load value of 7 Nm. In the case of dynamic load, no fault related finding was observed even in the case of 4 shorted turns. Because of the short duration of the transitions stay, it limits the number of recorded points, making the FFT analysis inadequate.

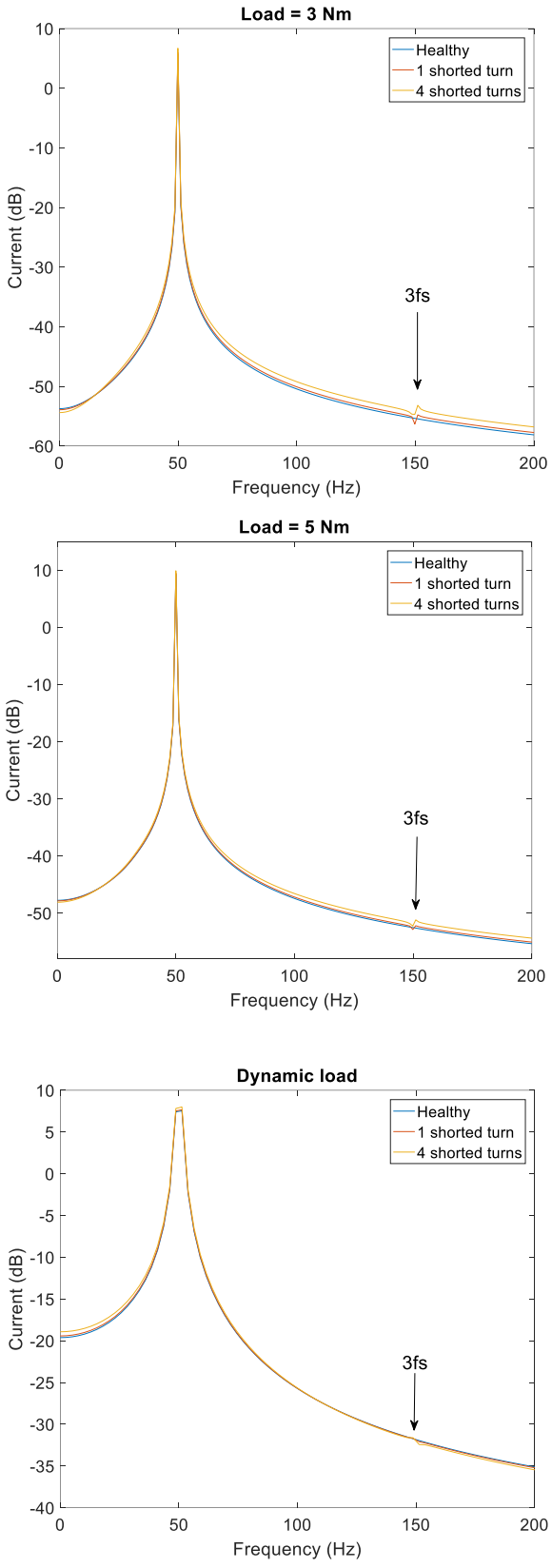

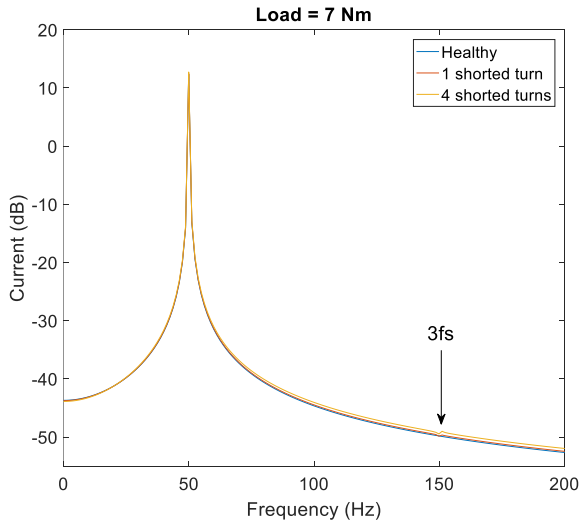

Fig.5. FFT motor current spectrum

Fig.6 displays the time-order representations for healthy and faulty induction motor obtained via the application of the AD-OT technique to the stator current signal for the following cases: healthy, 1 shorted turn and 4 shorted turns shown respectively in Fig. 6 (a), (b) and (c). The Kaiser windowing was adopted in this study.

In Fig.6 (a) we note the presence of a single time-varying order component corresponding to the fundamental component whose value can be calculated using the equation (16) as follow:

$$Order_{fundamental} = f_s . \left(60 / \omega_r \right)$$

By comparing the time-order representation for the faulty motor shown in (Fig.6 (b) and (c)) with that of healthy case (Fig.6 (a)) we can clearly see the apparition of a new time-varying order component (whose value is around the 3rd order, corresponding to the component $f_{sc_3} = 3.f_s$ in the frequency domain) at the instant t= 1s, whose amplitude increases as the fault severity increases. Using the equation (16), the exact value of the order component due to the ITSC fault can also be calculated as follow:

$$Order_{sc_3} = f_{sc_3} . \left(60 / \omega_r \right)$$

On the other hand, it is also noted that the value of these order components depends on the amount of load applied to the motor.

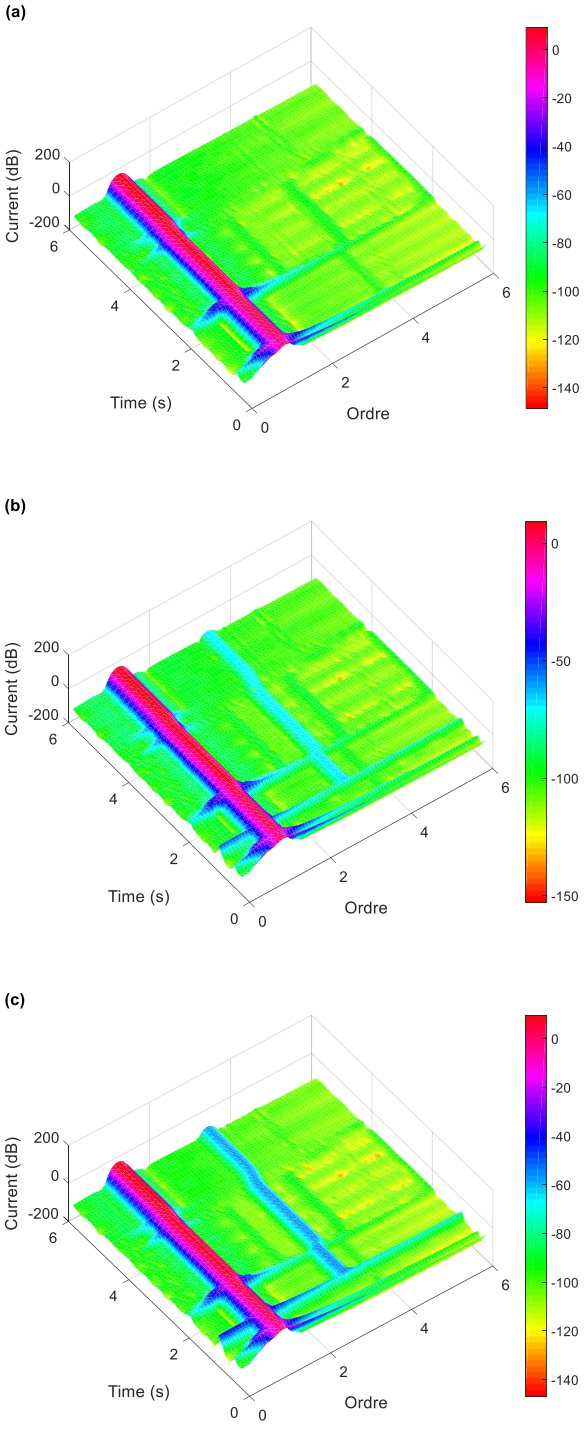

Fig. 6. AD-OT spectral map of the stator current, (a) healthy case, (b) faulty case (1 shorted turn at t = 1 s in phase *a*), (c) faulty case (4 shorted turns at t = 1 s in phase *a*)

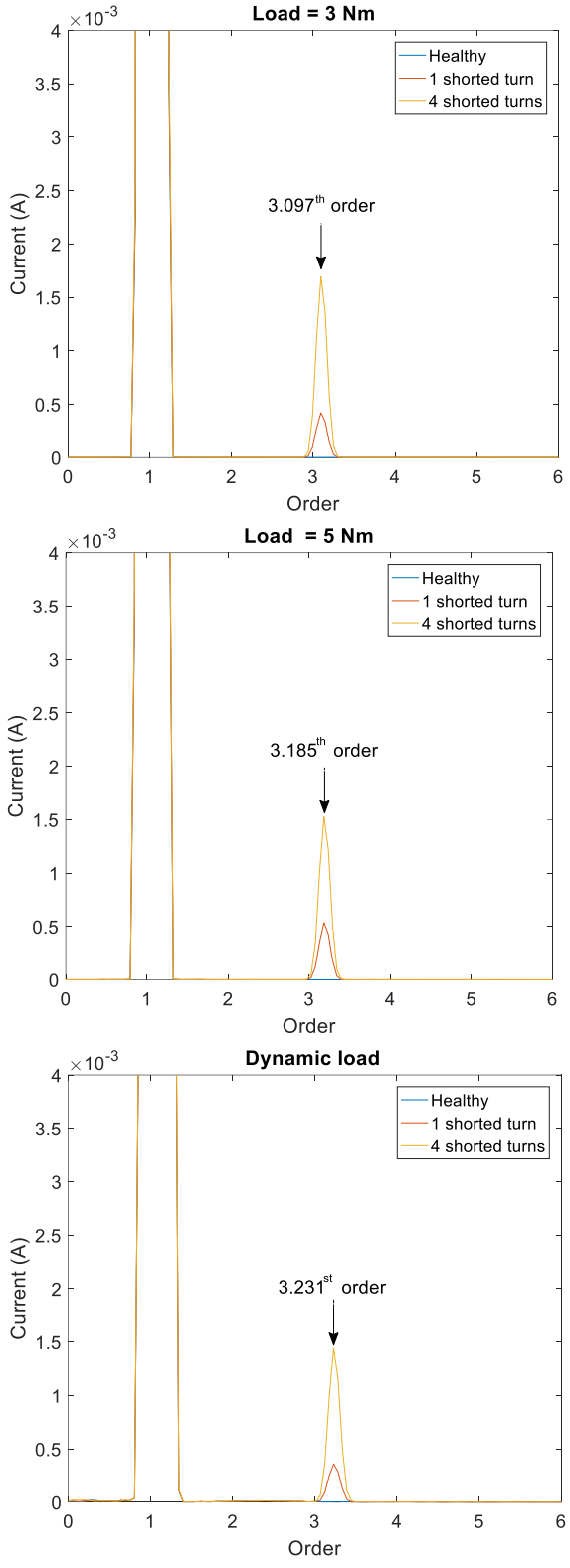

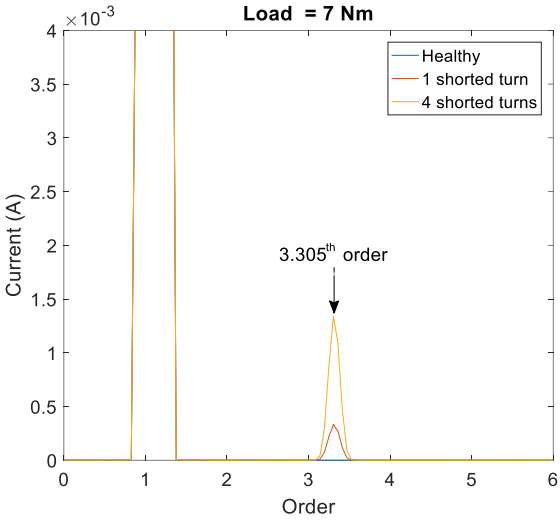

Fig. 7. AD-OT motor current spectrum

One of the highlights of the AD-OT technique is its ability to extract the information present in the signal with high precision at different times and for different operating modes. Fig. 7 shows the spectrum of the stator current obtained with the AD-OT technique for different load levels. From this figure it can clearly be seen that the ITSC fault gives rise to an order component whose values are 3.097, 3.185, 3.231 and 3.305 corresponding respectively to load level of 3 Nm, 5 Nm, dynamic load and 7 Nm. The amplitude of this order component increases with the degree of the defect. On the other hand, it is observed that the AD-OT technique is not affected by the transient state caused by the dynamic load applied to the motor.

5. Conclusion

In this study the Angular Domain Order Tracking (AD-OT) technique was applied on the induction motor current signal for detecting inter-turn short-circuit (ITSC) fault and compared with the classical Fourier analysis (FFT).

Our main goal was to test the ability of the AD-OT technique to detect the ITSC fault under non-stationary conditions.

The obtained results demonstrated the efficiency of the AD-OT technique for the detection of ITSC fault under varying load conditions and this even for 1 shorted turn.

On the other hand, the diagnostic procedure of the AD-OT technique is simple and accurate since it is sufficient to monitor the evolution of the 3^{rd} order component corresponding to the $3.f_s$ component in the frequency domain.

Appendix

Tab.1. Induction motor parameters

P_n	output power	1.1 KW
V_s	stator voltage	220 V
f_s	stator frequency	50 Hz
p	number of pole pairs	1
R_s	stator resistance	7.828 Ω
R_b	rotor bar resistance	0.15 mΩ
R_e	resistance of end ring segment	0.072 mΩ
L_b	rotor bar inductance	0.1 µH
L_e	inductance of end ring	0.1 µH
L_{sf}	leakage inductance of stator	0.018 H
N_s	number of turns per stator phase	160
N_b	number of rotor bars	16
l	length of the rotor	65 mm
e	air-gap mean diameter	2.5 mm
i	inertia moment	6.093 10^{-3} kg.m^2

References

1. Trigeassou, J.C., ed.: *Electrical Machines Diagnosis.* John Wiley & Sons, 2013.
2. Riera-Guasp, M., Antonino-Daviu, J. A., Capolino, G. A.: *Advances in electrical machine, power electronic, and drive condition monitoring and fault detection: State of the art*. In : IEEE Transactions on Industrial Electronics, 2015, vol. 62, no 3, p. 1746-1759.
3. Bouzid, M. B. K., Champenois, G.: *New expressions of symmetrical components of the induction motor under stator faults*. In : IEEE Transactions on Industrial Electronics, 2013, vol. 60, no 9, p. 4093-4102.
4. Lahoud, N., Faucher, J., Malec, D., & Maussion, P.: *Electrical aging of the insulation of low-voltage machines: Model definition and test with the design of experiments*. In: IEEE Transactions on Industrial Electronics, 2013, vol. 60, no 9, p. 4147-4155.
5. Bouzid, M. B. K., Champenois, G., Bellaaj, N. M., Signac, L., Jelassi, K.: *An effective neural approach for the automatic location of stator interturn faults in induction motor*. In: IEEE Transactions on Industrial Electronics, 2008, vol. 55, no 12, p. 4277-4289.
6. Sahraoui, M., Ghoggal, A., Guedidi, S., Zouzou, S. E.: *Detection of inter-turn short-circuit in induction motors using Park–Hilbert method*. In: International Journal of System Assurance Engineering and Management, 2014, vol. 5, no 3, p. 337-351.
7. Henriquez, P., Alonso, J. B., Ferrer, M. A., Travieso, C. M.: *Review of automatic fault diagnosis systems using audio and vibration signals*. In : IEEE Transactions on Systems, Man, and Cybernetics: Systems, 2014, vol. 44, no 5, p. 642-652.
8. Singh, G., Kumar, T. C. A., Naikan, V. N. A.: *Induction motor inter turn fault detection using infrared thermographic analysis*. In: Infrared Physics & Technology, 2016, vol. 77, p. 277-282.
9. Jung, J. H., Lee, J. J., & Kwon, B. H.: *Online diagnosis of induction motors using MCSA*. In : IEEE Transactions on Industrial Electronics, 2006, vol. 53, no 6, p. 1842-1852.
10. Benbouzid, M. E. H.: *A review of induction motors signature analysis as a medium for faults detection.* In: IEEE transactions on industrial electronics, 2000, vol. 47, no 5, p. 984-993.
11. Mehala, N., Dahiya, R.: *Condition monitoring methods, failure identification and analysis for Induction machines*. In: International journal of circuits, systems and signal processing, 2009, vol. 3, no 1, p. 10-17.
12. Sakhara, S., Saad, S., Nacib, L.: *Diagnosis and detection of short circuit in asynchronous motor using three-phase model*. In : International Journal of System Assurance Engineering and Management, 2014, vol. 7, no 3, p. 1-10.
13. Benbouzid, M. E. H., Kliman, G. B.: *What stator current processing-based technique to use for induction motor rotor faults diagnosis?*. In: IEEE Transactions on Energy Conversion, 2003, vol. 18, no 2, p. 238-244.
14. Kechida, R., Menacer, A., Talhaoui, H., & Cherif, H.: *Discrete wavelet transform for stator fault detection in induction motors*. In: Diagnostics for Electrical Machines, Power Electronics and Drives (SDEMPED), 2015 IEEE 10th International Symposium on. IEEE, 2015. p. 104-109.
15. Gandhi, A., Corrigan, T., Parsa, L.: *Recent advances in modeling and online detection of stator interturn faults in electrical motors*. In: IEEE Transactions on Industrial Electronics, 2011, vol. 58, no 5, p. 1564-1575.
16. Akar, M.: *Detection of a static eccentricity fault in a closed loop driven induction motor by using the angular domain order tracking analysis method*. In: Mechanical Systems and Signal Processing, 2013, vol. 34, no 1, p. 173-182.
17. Blough, J. R.: *A survey of DSP methods for rotating machinery analysis, what is needed, what is available*. In: Journal of sound and vibration, 2003, vol. 262, no 3, p. 707-720.
18. Brandt, A.: *Noise and vibration analysis: signal analysis and experimental procedures*. John Wiley & Sons, 2011.
19. Laribi, S. S., Champenois, G., Bendiabdellah, A., Meradi, S.: *Bar faults diagnosis of an indirect vector control squirrel cage induction motor*. In: Electrical Engineering and Software Applications (ICEESA), 2013 International Conference on. IEEE, 2013. p. 1-6.
20. Gentile, G., Meo, S., Ometto, A.: *Induction motor current signature analysis to diagnostics, of stator short circuits*. In: Diagnostics for Electric Machines, Power Electronics and Drives, 2003. SDEMPED 2003. 4th IEEE International Symposium on. IEEE, 2003. p. 47-51.
21. Talhaoui, H., Menacer, A., Kessal, A., Kechida, R.: *Fast Fourier and discrete wavelet transforms applied to sensorless vector control induction motor for rotor bar faults diagnosis*. In: ISA transactions, 2014, vol. 53, no 5, p. 1639-1649.
22. Akbari, H., Meshgin-Kelk, H., Milimonfared, J.: *Induction machine modeling including the interbar currents using winding function approach*. In: International Review of Electrical Engineering-IREE, 2009, vol. 4, no 2, p. 269-277.
23. Schaeffer, E.: *Diagnostic des machines asynchrones:*

Modèles et outils paramétriques dédiés à la simulation et à la détection de défauts. Ph.D. dissertation, Université de Nantes, Nantes, France, 1999.
24. Bachir, S., Tnani, S., Trigeassou, J. C., Champenois, G.: *Diagnosis by parameter estimation of stator and rotor faults occurring in induction machines*. In: IEEE Transactions on Industrial Electronics, 2006, vol. 53, no 3, p. 963-973.
25. Bazine, I. B. A., Tnani, S., Poinot, T., Champenois, G., Jelassi, K.: *On-line detection of stator and rotor faults occurring in induction machine diagnosis by parameters estimation*. In: Diagnostics for Electric Machines, Power Electronics & Drives (SDEMPED), 2011 IEEE International Symposium on. IEEE, 2011. p. 105-112.